Experimental verification of a GPS network: characterization and removal of multipath effects

Michael Kochly[*a], Tracy Kijewski-Correa[a]
[a]Dept. of Civil Eng., University of Notre Dame, 156 Fitzpatrick Hall, Notre Dame, IN, USA 46556

ABSTRACT

The aging Civil Infrastructure System (CIS) in the United States has prompted the need for more effective structural health monitoring (SHM) techniques. Global Positioning Systems (GPS) have shown great promise for SHM, as they allow the total displacement of a structure to be measured, unlike other traditional sensors (i.e. accelerometers and strain gages). However, past research efforts have shown GPS to suffer from the effects of multipath interference, greatly reducing its accuracy in urban areas. In this study, a testing program was developed in which a controlled multipath source was introduced into a GPS network to allow for the characterization and removal of this phenomenon. In addition, the GPS performance was benchmarked against two more widely accepted sensor technologies: a terrestrial positioning system (TPS) and an accelerometer, to demonstrate its utility for monitoring CIS.

Keywords: Structural health monitoring, GPS, multipath effects

1. INTRODUCTION

The United States' aging Civil Infrastructure System (CIS) imposes a significant economic burden, not only in the cost of repairs themselves, but also in the lengthy closure times to complete repairs. Hence, it is critical that repairs be made proactively to minimize these burdens and keep the nation's infrastructure well-maintained and in safe operating condition. Structural health monitoring (SHM) allows potential problems to be diagnosed and repaired before they warrant the complete closure of critical infrastructure. In addition, SHM can be used for rapidly assessing structures after natural disasters, such as earthquakes (BORP, 2003 and Celebi et al., 2004), comparing in-situ response with design predictions and monitoring changes in a structure over time, such as softening or settlement.

Traditionally, SHM has been accomplished through the use of accelerometers or strain gages. While simple and inexpensive, these sensors have a noteworthy drawback: they are unable to capture the complete global response of a structure. Hence, crucial information, such as the mean and background components of wind-induced response, settlement, permanent offsets resulting from significant damage and thermal expansion, cannot be obtained through the use of these sensors. These quantities can be important to completely characterize a structure's condition in an SHM framework thus requiring the integration of global displacement sensors, such as terrestrial positioning systems (TPS) and microwave interferometer. Unfortunately, these technologies suffer from line-of-sight issues with accuracies degrading in foggy, hazy and stormy conditions. Global Positioning Systems (GPS) provide an alternate global displacement sensing technology for SHM, capable of continuous, unattended operation in all weather conditions.

GPS directly provides the global displacement of a structure along two perpendicular axes and in the vertical direction. Additionally, sampling rates of up to 20 Hz and sub-centimeter accuracy levels have made these sensors capable of monitoring a wide range of structures. GPS technology has been utilized in several full-scale SHM programs to date, including the works of: Celebi and Sanli (2002) in San Francisco and Los Angeles, Chen et al. (2001) on the Di Wang Building in China, Tamura et al. (2002) on a tower in Tokyo, Park et al. (2004) on a 66-story building in Korea, Brownjohn et. al (2003) on Singapore's Republic Plaza and the work of the second author on a high-rise building in Chicago (Kijewski-Correa and Kareem, 2003).

[*]mkochly@nd.edu; phone 1 574 631 3914; http://www.nd.edu/~dynamo/

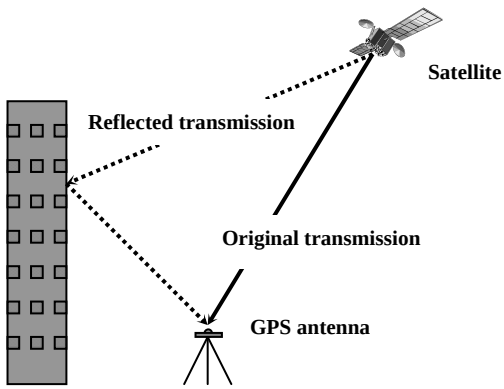

Figure 1: Generation of multipath error.

The above research efforts have shown the great promise of GPS technology but have also highlighted the damaging effects caused by multipath. Multipath occurs when GPS satellite signals are bounced off of reflective objects and arrive at the GPS antenna after the original transmission, as illustrated in Figure 1. This introduces a long period distortion into the GPS measurements. Multipath can be responsible for errors of up to several meters in the satellite pseudoranges (Evans and Hermann, 1990), thus making it the largest error source that cannot be removed through differential GPS (DGPS) processing, a technique involving the use of two GPS receivers— a stationary reference and a rover. Additionally, heavily congested urban areas, where most SHM applications take place, are especially prone to multipath due to the large concentration of reflective objects. As such, characterizing multipath and developing a scheme for its removal is critical. Two unique features of multipath can be exploited to aid in characterization. First, multipath effects produce long-period distortions in GPS position estimates well below the fundamental frequency of Civil structures, which appear at varying amplitudes in both orthogonal position estimates. Secondly, since the GPS satellites complete their orbit approximately once every 24 hours, while the reflective objects causing multipath are fixed, the same spurious long period trends should reappear daily in the GPS position estimates. Both of these features have been utilized by the authors in this study to diagnose multipath effects using a GPS network established at the University of Notre Dame complete with a reflective sheet used to induce a controlled multipath signature into the data. The performance of a GPS sensor within this network was also compared to two traditional sensors— an accelerometer and a TPS. This paper discusses these efforts with specific focus on the characterization and subsequent removal of the observed multipath effects.

2. CALIBRATION STUDY

In order to fully verify GPS as a suitable technology for SHM, a comprehensive calibration study was performed at the University of Notre Dame. A GPS network was established, consisting of a reference and two rover stations and located in an open area with a clear view of the sky. The rover sites utilized Leica SR530 receivers, while the reference site was equipped with a Leica GRX1200 model. Both of these sensors have dual frequency (L1 and L2) technology and are capable of logging up to twelve incoming satellite transmissions. While the GRX1200 has a maximum sampling rate of 20 Hz, the GPS network was constrained to a sampling rate of 10 Hz, the maximum rate of the SR530 receivers. Leica AT504 choke ring antennas were employed at both rover stations. The four concentric choke rings of these antennas reduce the amount of multipath interference by blocking out signals arriving at low elevations and from beneath the ground plane, though signals arriving at high elevations can still be received. At the reference site, a newly released SmartTrak antenna was used, featuring sub-millimeter phase accuracy. By utilizing a stationary reference site in conjunction with the rover sites, DGPS sensing was possible. The use of DGPS eliminates the majority of the errors inherent to GPS monitoring, including atmospheric and receiver clock errors, resulting in a sub-centimeter accuracy level. For more information on the theory of GPS refer to Seeber (1993).

In addition to the GPS units, two traditional SHM sensors were utilized in order to benchmark the GPS performance: a TPS and an accelerometer. A Leica TPS1200 was used in conjunction with a 360° prism. The TPS1200 has a rotating motor, allowing it to track dynamic motions to an accuracy of 5mm. The accelerometer employed was piezoelectric with a sensitivity of 1.015 V/g, whose recorded accelerations were integrated twice to obtain a dynamic

displacement estimate. Note that by design this type of accelerometer has a frequency response function (FRF) that tends to roll off at frequencies below 0.5 Hz, making it unable to capture low frequency signals.

All three sensors were used to track motions imparted by a small, deployable shake table, simulating signals ranging from simple sine waves to building motions under the action of wind and earthquakes. While a total of over 50 tests were performed, for brevity only two will be discussed herein: a sine wave of amplitude ±3 cm and frequency of 1 Hz and the tracking of the wind-induced response of a high-rise steel building in Chicago.

2.1 Sine wave test

By tracking several sine waves of varying amplitude and frequency, the dynamic limits of the sensors could be gauged. For the test considered here, a sine wave of amplitude ±3 cm and frequency of 1 Hz, the three sensors were compared relative to the shake table command signal and their performance was gauged by the following metrics: the RMS value (σ), minimum (x_{min}) and maximum (x_{max}) values and the average of the local maxima and minima values. The average maxima ($\bar{\varepsilon}_{max}$) and minima values ($\bar{\varepsilon}_{min}$) quantify each sensor's ability to capture each peak of a signal, and are computed, as defined in equation 1 for the case of local maxima:

$$\bar{\varepsilon}_{max} = \frac{\sum_{i=1}^{N} 100 * \frac{\left| max_{i,sensor} - max_{i,shake} \right|}{max_{i,shake}}}{N} \tag{1}$$

where $max_{i,\ sensor}$ = ith local maxima of the sensor (GPS, TPS or accelerometer), $max_{i,\ shake}$ = ith local maxima of the shake table and N = number of local maxima. This yields a more robust representation of sensor performance in comparison to point estimates like the global maximum and minimum values and is analogous to the RMS value for local signal extrema. Statistics for this test are tabulated in Table 1 and a snapshot of the time history is shown in Figure 2. The GPS sensor performed extremely well relative to the other sensors, as it had the lowest RMS and average maxima and minima errors. From the time history, it can be observed that the TPS suffers from phase distortion at this frequency of motion.

Table 1: Statistics from sine wave test

	RMS (cm)	% Diff	Max (cm)	% Diff	Min (cm)	% Diff	$\bar{\varepsilon}_{max}$ (%)	$\bar{\varepsilon}_{min}$ (%)
Shake Table	2.07	--	2.98	--	-2.97	--	--	--
GPS	2.09	0.8	3.36	12.6	-3.45	15.7	5.1	4.8
TPS	2.10	1.4	3.96	32.6	-3.94	32.0	42.3	38.4
Accelerometer	1.93	6.8	2.81	5.4	-2.81	5.4	8.7	8.8

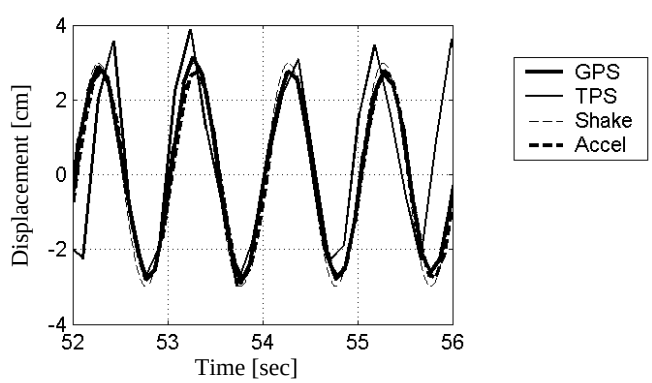

Figure 2: 10-second snapshot of time history for a sine wave of amplitude ±3 cm and frequency of 1 Hz.

2.2 Full-scale data test

The next test investigates the tracking ability of the sensors using full-scale data collected by the GPS deployed on a high-rise steel building as part of the Chicago Full-Scale Monitoring Program (Kijewski-Correa, 2003; Kijewski-Correa et al., 2005). Thus, actual full-scale displacements measured by GPS were used as inputs to the shake table. By using a full-scale measured displacement time history under the action of wind, the time series includes both the background and resonant components of the response. The displacement time history and its power spectral density (PSD) are shown in Figure 3, with the statistics tabulated in Table 2. Note that this low frequency response is outside the operating range of the accelerometer, as alluded to previously. Hence, only the shake table and the results from the GPS and TPS sensors are presented. Overall, the GPS does an excellent job of tracking the shake table motion and has a smaller RMS error than that of the TPS sensor. In addition, the PSD in Figure 3 shows that both the GPS and TPS performed well in identifying the energy content in the signal with a resonant peak at 0.14 Hz, which matches the prediction from finite element models used in their design (Kilpatrick et al., 2003). Note also that the GPS and TPS sensors were able to capture the background component of the response, which is characterized by the low-frequency spectral content in the PSD.

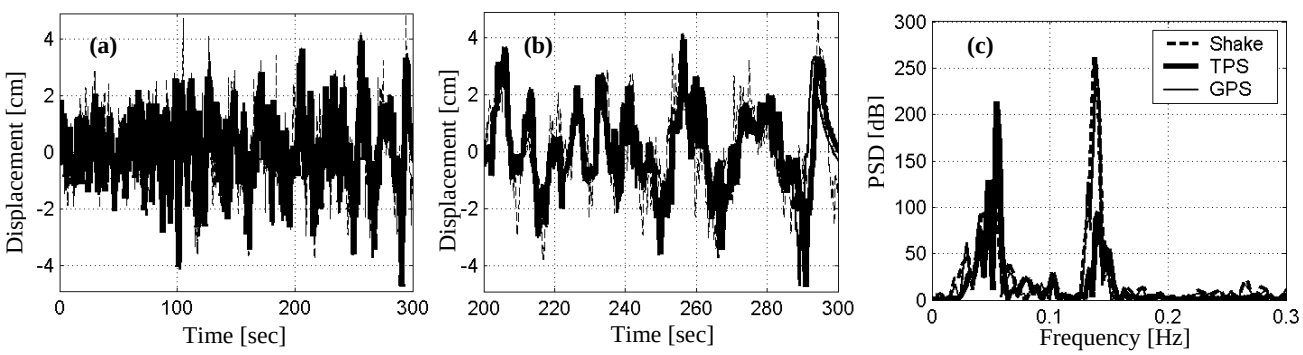

Figure 3: (a) Time history of high-rise steel building from full-scale data, (b) zoom-in from 200-300 s and (c) PSD.

Table 2: Statistics from full-scale high-rise steel building test

	RMS (cm)	% Diff	Max (cm)	% Diff	Min (cm)	% Diff	$\bar{\varepsilon}_{max}$ (%)	$\bar{\varepsilon}_{min}$ (%)
Shake Table	1.32	--	5.01	--	-3.90	--	--	--
GPS	1.25	5.4	3.95	21.2	-4.72	21.0	33.3	35.1
TPS	1.24	6.0	4.13	17.6	-4.71	20.8	33.3	30.7

3. CHARACTERIZATION AND REMOVAL OF MULTIPATH

Despite the numerous advantages of GPS for use in SHM and its strong performance in the benchmark tests discussed in the preceding section, there is still one factor that severely limits its utility in dense urban zones: multipath errors. As previously discussed, multipath represents the largest remaining error source for GPS monitoring in urban zones and causes significant distortions in the data, an example of which is shown in Figure 4. Previous efforts have been made to remove multipath effects using wavelet-based approaches (Chen et al., 2001) and a simple high-pass filter technique (Kochly et al, 2005). While the latter effort produced much cleaner time histories, this brute force approach resulted in the removal of the mean component and may have diminished the background component of wind-induced response. This motivated an attempt to find a time domain removal strategy, which is presented herein. In order to first characterize the multipath, further field tests were conducted in which an aluminum sheet was deployed to induce multipath, as depicted in Figure 5, in a controlled setting so that a removal scheme could be developed. The following sections will detail the controlled multipath test, the results of the test and the removal scheme developed.

3.1 Multipath test

To investigate the multipath phenomenon, a stationary test was performed in which an aluminum reflector was introduced near the rover antenna. The reflector was placed 32 feet to the North of the receiver (see Figure 5), as the majority of the GPS satellites ascend along a North to South trajectory. Thus, this placement ensured that the reflector

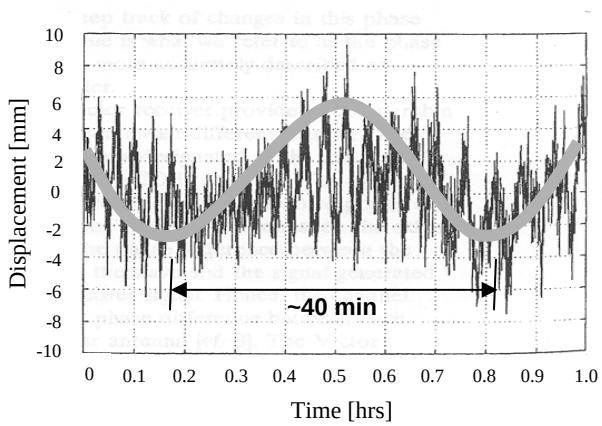

Figure 4: Example of a multipath signature in GPS recorded data (adapted from Axelrad et al., 1996).

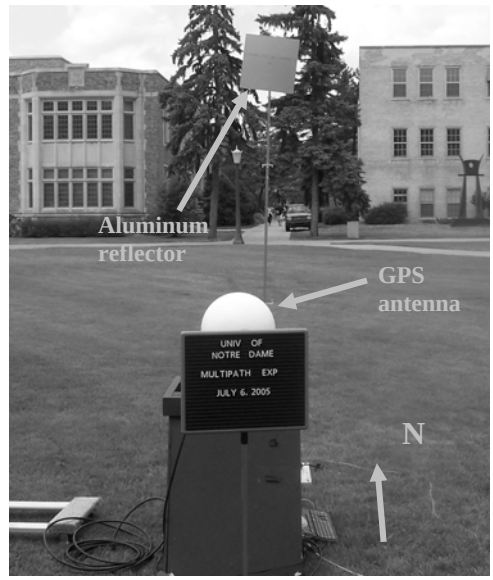

Figure 5: Aluminum reflector used to induce multipath effects.

would interfere with as many satellite transmissions as possible. With the rover antenna kept stationary, data was then logged for 48-hours continuously. As such, any "motion" detected by the unit is evidence of inherent errors in the system. By collecting data over a period of two consecutive days, the repeatability of the satellite constellations, which repeat 4 minutes earlier each day (the so-called sidereal day), could be exploited. Hence, every potential satellite configuration was observed twice over the duration of this test and any harmonic components that appeared in both days could be safely attributed to multipath, thus allowing a multipath signature to be established for the site. Results from the 48 hour static test are presented in the subsequent section.

3.2 Multipath test results

The complete test results for the 48-hour test cannot be included here due to space constraints. Instead, a time history for one three-hour block from the test is shown in Figure 6, with the results from the second sidereal day plotted atop those from the first sidereal day. The relative displacements detected by the GPS antenna are presented and, as the GPS receiver defines its positions in a local coordinate system of Northings and Eastings, all results are plotted in terms of the North-South (N-S) and East-West (E-W) displacements. Examining Figure 6, it can be seen that both the N-S and E-W displacements exhibit long-period trends that are repeated over both sidereal days.

In order to determine the presence of multipath errors, a Fourier analysis was first carried out. The 48-hour test was divided into sixteen three-hour blocks, with each being analyzed using a PSD to identify low frequency components induced by multipath. By examining both the E-W and N-S PSDs, those low frequency distortions which manifested

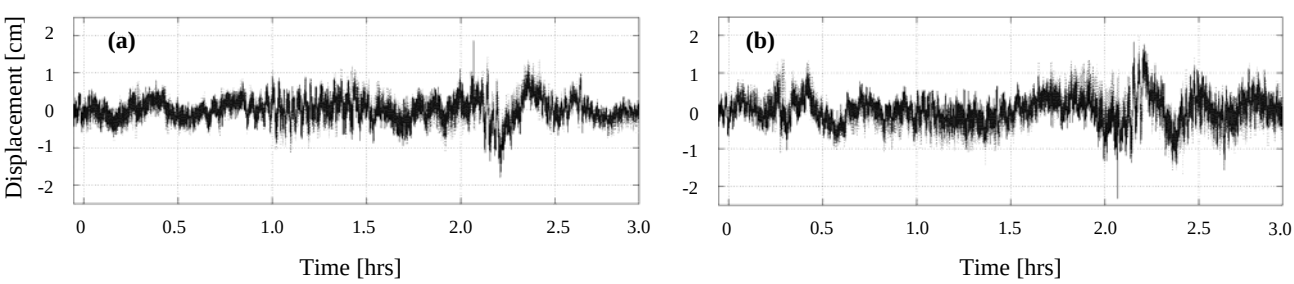

Figure 6: 3-hour period from 48-hour static test: (a) E-W displacement and (b) N-S displacement. Results from 2nd sidereal day (dashed) plotted atop results from 1st sidereal day (solid).

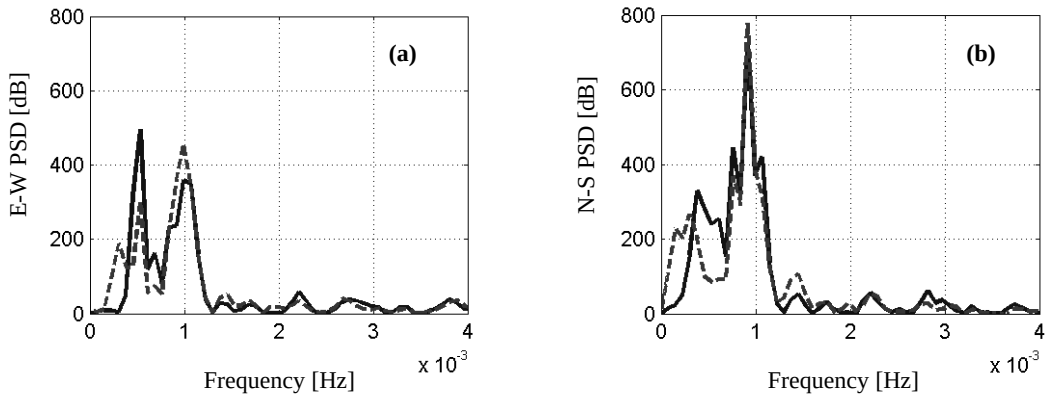

Figure 7: PSD of 3-hour block of GPS static displacements for (a) E-W and (b) N-S directions with results from 2nd sidereal day (dashed) plotted atop those from 1st sidereal day (solid).

themselves over the course of both sidereal days and in both response directions could be attributed to multipath interference, as discussed previously. One such PSD is presented in Figure 7 for the same three-hour block in Figure 6. For this particular three-hour block, the E-W and N-S directions both share a common low frequency component at approximately 0.00099 Hz, corresponding to a period of about 17 minutes, which appears during both days of testing.

Upon conducting similar analyses for the remaining three-hour blocks, it was found that there were several large, low frequency components that appeared in both response directions and over the course of both days during the 48-hour test. These components are listed in Table 3, with the time (in hours) referring to the elapsed time from the start of the static test. Note that the time is listed for both the first and second days of the test, i.e. hours 7 to 9 on the first day correspond to hours 31 to 33 on the second day. Note that the identified multipath components do not remain at the same frequency for each three hour block, but tend to oscillate. However, small fluctuations in periodicity are expected for multipath interferences, as the phenomenon itself is non-stationary due to the continuous orbit of satellites overhead. As the satellite configurations are constantly changing, the paths of the reflected signals are altered and, thus, the arrival time of the reflected transmission at the GPS receiver varies. As can be seen from Table 3, the multipath periodicities for this test range from 15 to 20 minutes, which is within the range of values found in other GPS studies (e.g., Axelrad, 1996). With the multipath interference now diagnosed, the next section will detail the efforts to remove it from the GPS positions.

Table 3: Observed Multipath Frequencies and Periods for 48-hour Static Test

Elapsed Time: 1st day / 2nd day (Hrs)	Frequency (Hz)	Period (min)
1-3 / 25-27	0.001068	16
7-9 / 31-33	0.000992	17
10-12 / 34-36	0.001140	15
13-15 / 37-39	0.000839	20
19-21 / 43-45	0.000839	20
22-24 / 46-48	0.000992	17

3.3 Multipath removal

To remove the traces of multipath from the GPS measured displacements, a multipath signature was first generated for the entire 48-hour static test. This signature was created by fitting each three-hour time history with a polynomial curve utilizing a least squares approach. The least squares method is a common scheme for removing trends in data sets and a description of the technique can be found in numerous texts, e.g., Bendat and Piersol (1986). A brief discussion of the procedure used follows. The polynomial fit to the original GPS position data u is given by:

$$\bar{u} = \sum_{k=0}^{K} b_k \left(n\Delta t\right)^k \qquad n = 1, 2, ..., N \tag{2}$$

where $\bar{u}$ = polynomial/multipath error fit, K = degree of polynomial, b_k = regression coefficients, Δt = time step and N = the number of data points in the original data set. The least squares method then formulates the best possible fit to the original data by minimizing the squared differences Q between the original data u and the polynomial fit $\bar{u}$ as shown below:

$$Q = \sum_{n=1}^{N} b_k \left(u - \bar{u}\right)^2 \tag{3}$$

Q is minimized by taking the partial derivatives of Q with respect to b_k and equating them to zero. This results in $K+1$ equations of the following form:

$$\sum_{k=0}^{K} b_k \sum_{n=1}^{N} (n\Delta t)^{k+m} = \sum_{n=1}^{N} u(n\Delta t)^m \quad m = 0,1,2,...K \tag{4}$$

Using equation 4, the regression coefficients b_k can be obtained. Once the regression coefficients are known, the entire polynomial fit/multipath signature $\bar{u}$ can be assembled.

As the time histories for this test are lengthy and characterized by numerous frequency components, a high order polynomial was required to accurately capture the multipath distortion. A trial and error approach was used to determine the best order polynomial to use, with a range of 30 to 60 considered. Within this range, the optimal order was defined as that which minimizes the RMS error of the representation. By iterating upon the order number, a 55th order polynomial was deemed necessary to model the multipath effects. Figure 8 shows the multipath signatures obtained for the E-W and N-S directions from the polynomial curve fitting procedure for the same three-hour block presented previously. From this figure it can be seen that the least squares approach effectively captures the long period trends and large swings in the data caused by multipath, whose distortions exceed 0.5 cm for this particular three-hour block. Analyses of the remaining three-hour blocks were carried out in a similar fashion, with multipath errors as large as 1 cm being observed. For more reflective environments, such as dense urban zones, it is likely that the magnitude of this error will be even more pronounced and additional harmonics will be observed.

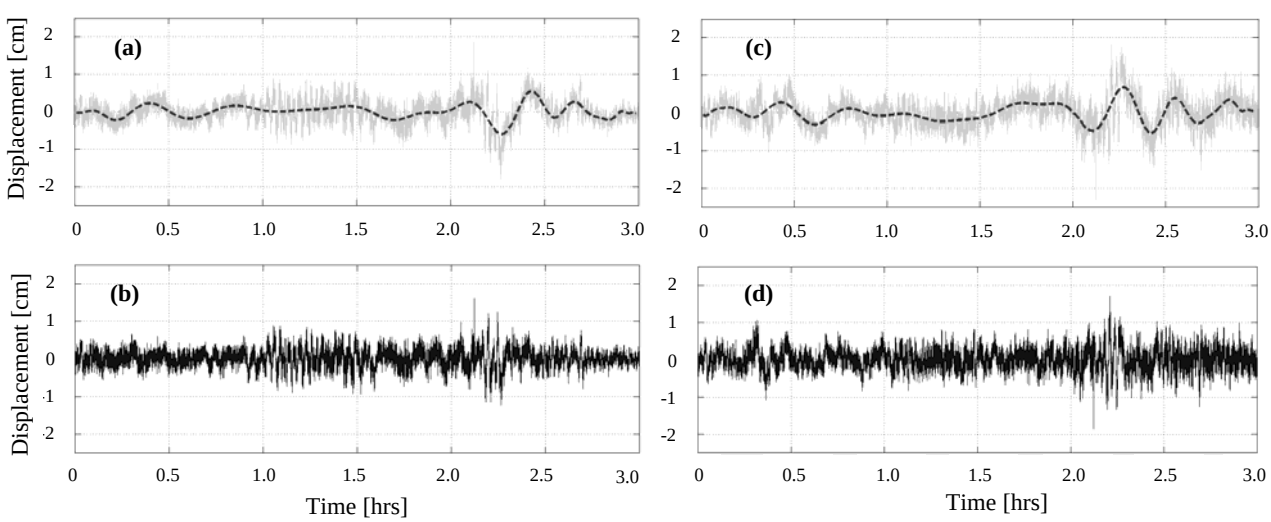

Figure 8: Multipath signatures and filtered responses: (a) Multipath signature (dashed line) for E-W response, (b) Detrended E-W response, (c) Multipath signature (dashed line) for N-S response, (d) Detrended N-S response.

Once the multipath signature was obtained for the entire 48-hour test, the GPS static data was filtered by subtracting the polynomial curve fits from the original GPS position estimates, as shown in Equation 5:

$$u_{new} = u - \bar{u} \tag{5}$$

with u_{new} = the detrended response. Upon removing the long period trends induced by multipath, a much cleaner time history is observed, as shown in Figure 8, with a more random characteristic indicative of the broadband background noise documented in the sensor by Kijewski-Correa (2003).

The effect of the multipath removal scheme can also be quantified statistically. The standard deviations for each three-hour time history were calculated before and after the removal procedure and are tabulated for both response directions in Table 4. These results clearly demonstrate the drastic improvement produced by the removal scheme, as the standard deviations for both response directions are reduced by an average of over 20%. Also, note that the N-S position estimate has a higher noise level as compared to that of the E-W position, with standard deviations that are, on average, 1.7 times larger. This degradation in accuracy is most likely due to the fact that the GPS satellites ascend along a N-S trajectory, making the psuedoranges for this direction more difficult to ascertain. Following the removal operation, the average RMS value for both response directions falls beneath the manufacturer's specified value of 0.3 cm for static tracking. In addition, the RMS values of the detrended response are comparable to RMS values obtained through static testing performed without the presence of the reflector (Kijewski-Correa, 2003).

With the multipath signature now acquired for one sidereal day, for any future monitoring conducted with the GPS antennas at this site, the multipath error can be eliminated by simply subtracting out the multipath error polynomial $\bar{u}$ for the appropriate time window under consideration. This procedure will reduce the large swings in position common to multipath errors, hence lowering the standard deviation of the results as shown through these test results. For full-scale deployments, this procedure can be adapted in order to obtain a multipath model prior to the start of monitoring by recording 48 hours of consecutive data under low wind conditions to establish the static baseline for the sensor.

Table 4: Standard Deviations of GPS Position Data from Static Multipath Test-
Before and After Multipath Removal

Elapsed Time [Hrs]	E-W Response			N-S Response		
	σ_{before} [cm]	σ_{after} (cm)	% Diff	σ_{before} [cm]	σ_{after} (cm)	% Diff
1-3	0.199	0.164	17.5	0.259	0.235	9.5
25-27	0.205	0.156	24.1	0.273	0.233	14.6
4-6	0.217	0.170	21.6	0.260	0.231	11.3
28-30	0.225	0.167	25.6	0.255	0.223	12.6
7-9	0.301	0.233	22.5	0.364	0.278	23.7
31-33	0.325	0.243	25.3	0.435	0.304	30.1
10-12	0.217	0.145	33.2	0.345	0.252	26.9
34-36	0.242	0.145	40.3	0.381	0.254	33.4
13-15	0.166	0.136	17.8	0.287	0.236	17.7
37-39	0.180	0.131	27.0	0.360	0.235	34.6
16-18	0.249	0.209	15.9	0.384	0.332	13.7
40-42	0.254	0.209	17.5	0.537	0.319	40.7
19-21	0.205	0.161	21.8	0.555	0.451	18.7
43-45	0.227	0.166	26.7	0.634	0.533	16.0
22-24	0.210	0.159	24.4	0.332	0.247	25.5
46-48	0.207	0.155	25.4	0.303	0.240	20/9
AVERAGE	0.227	0.172	24.2	0.373	0.288	22.8

4. CONCLUSIONS

For structural health monitoring to be effective, it is crucial that the sensors used are highly accurate and can provide the necessary response quantities, including total displacements. GPS sensors offer a promising tool for these purposes, capable of continuous and unattended operation. In addition, the benchmark tests performed demonstrate that a GPS network is as accurate (if not more so) than more traditionally used SHM sensors, such as accelerometers and TPS. One serious drawback to GPS monitoring in urban areas, though, is the effect of multipath errors. This paper introduced an approach to eliminate multipath effects by fitting the multipath error from a static GPS test using a least squares method. This error source can then be subtracted from the GPS measured positions to obtain the structural response. Applying this procedure yielded an improvement of over 20% in the quality of GPS RMS displacement estimates. By extending the multipath removal strategy to full-scale applications, the largest remaining error source for GPS monitoring in urban zones can be eradicated.

ACKNOWLEDGEMENTS

The authors are grateful to the University of Notre Dame and Leica Geosystems for its support of this research. In addition, the authors wish to thank Leica and Kara Corporation staff, James Stowell, Ryan Leonard, Robert Asher and Michael Carlyle, for their technical support and efforts. Lastly, the authors thank undergraduate researchers Kevin Haas, Peter Sweeney, and Andrew Descary for their help with experimental setup and data processing.

REFERENCES

1) Axelrad, P., Comp, C.J. and P.E. Macdoran (1996) "SNR-Based Multipath Error Correction for GPS Differential Phase," *IEEE Transactions on Aerospace and Electronic Systems,* 32(2): 650-659
2) BORP (2003) Building Occupancy Resumption Program, Department of Inspection, City of San Francisco, www.seaonc.org/pdfs/BORP%20Guidelines.pdf
3) Bendat, J. and Piersol, A. (1986), *Random Data: Analysis and Measurement Procedures*. John Wiley and Sons, New York.
4) Brownjohn, J.M.W. (2003) "Sensor and data management technology for structural health monitoring of civil structures," *Structural Health Monitoring and Intelligent Infrastructure*, Wu and Abe, Eds., Swets and Zeitlinger, Lisse, 1235-1241
5) Celebi, M. and A. Sanli (2002) "GPS in Pioneering Dynamic Monitoring of Long-Period Structures," *Earthquake Spectra*, 18(1): 47-61
6) Celebi, M., Sanli, A., Sinclair, M., Gallant, S. and Radulescu, D. (2004) "Real-time seismic monitoring needs of a building owner – and the solution: a cooperative effort", *Earthquake Spectra*, 20(2), 333-346
7) Chen, Y., Huang, D. and Ding, X. (2001) "Measurement of vibrations of tall buildings with GPS: a case study, Health Monitoring & Management of Civil Infrastructure Systems," Chase and Aktan, Eds., 4337, 477-483
8) Evans, A. and Hermann, B. (1990) "A Comparison of Several Techniques to Reduce Signal Multipath from the Global Positioning System," *Global Positioning System: an Overview*, Bock, Leppard and Cedd, 74-81
9) Kijewski-Correa, T. (2003) *Full-Scale Measurements and System Identification: A Time-Frequency Perspective.* PhD Dissertation, Department of Civil Engineering and Geological Sciences, University of Notre Dame, Notre Dame, IN
10) Kijewski-Correa, T. and Kareem, A. (2003) "The height of precision," *GPS World*, September, 20-34
11) Kijewski-Correa. T., Kilpatrick, J., Kwon, D.K., Bashor, R., Young, B.S., Abdelrazaq, A., Galsworthy, J., Morrish, D., Sinn, R.C., Baker, W.F., Isyumov, N. and Kareem, A. (2005) "Full-Scale Validation of the Wind-Induced Response of Tall Buildings: Updated Findings from the Chicago Monitoring Project," *Americas Conference On Wind Enginering*, Louisiana State University, LA, 31 May-4 June
12) Kochly, M., Kijewski-Correa, T. and Stowell, J. (2005) "GPS Monitoring in Urban Zones: Calibration and Quantification of Multipath Effects," *Proceedings of SPIE Conference on Smart Structures and Materials/NDE for Health Monitoring and Diagnostics*, San Diego, CA, 6-10 March
13) Seeber, G. (1993) *Satellite Geodesy – Foundations, Methods and Applications*. Walter de Gruyter & Co., Berlin: 209-355
14) Tamura, Y., Matsui, M., Pagnini, L.-C. and A. Yoshida (2002) "Measurement of Wind-Induced Response of Buildings Using RTK-GPS," *Journal of Wind Engineering and Industrial Aerodynamics*, **90**: 1783-1793